International Journal of Climatology

International Journal of Climatology RMetS

RESEARCH ARTICLE

Beyond Annual Averages: Multi-Scale Rainfall Variability, Drought Indicators, and Seasonal Shifts Under a Changing Climate

Hui Wang[1] | Tirusew Asefa[1,2] | Vasubandhu Misra[3,4]

[1]Tampa Bay Water, Clearwater, Florida, USA | [2]Patel College of Global Sustainability, University of South Florida, Tampa, Florida, USA | [3]Department of Earth, Ocean, and Atmospheric Science, Florida State University, Tallahassee, Florida, USA | [4]Center for Ocean-Atmospheric Prediction Studies, Florida State University, Tallahassee, Florida, USA

Correspondence: Hui Wang (hwang@tampabaywater.org)

Received: 26 December 2025 | **Revised:** 18 February 2026 | **Accepted:** 20 February 2026

Keywords: CMIP6 | drought risk | Florida Peninsula | general circulation models (GCMs) | seasonal shifts

ABSTRACT

Understanding rainfall variability across multiple temporal scales, especially for regions with strong seasonality, is essential for anticipating hydrological risks under climate change. This study investigates how precipitation patterns in the Florida Peninsula may evolve under two CMIP6 climate scenarios (SSP2-4.5 and SSP3-7.0) across two future periods: a near-term window (2026–2055) and a mid- to late-century horizon (2056–2085) critical for long-range water resources planning. Simulations from 18 General Circulation Models (GCMs), bias-corrected against the North American Land Data Assimilation System (NLDAS), were analysed to assess annual totals, monthly climatology, drought indicators, and rainy-season onset and demise. Results show that while mean annual rainfall may remain stable or even increase in some regions, precipitation becomes more variable at monthly and seasonal scales. Increased coefficients of variation, more frequent exceedance of cumulative rainfall deficit thresholds, and more erratic rainy-season onsets indicate heightened drought risks despite little change in annual totals. Regional contrasts are pronounced, with northern Florida tending toward wetter futures with modest variability increases, whereas southern Florida shows stronger drying tendencies, greater variability, and higher vulnerability to seasonal deficits, especially under SSP3-7.0. These findings underscore the importance of adaptive, climate-informed, and region-specific strategies for water management that move beyond annual averages to account for short-term variability and persistent deficits across multiple scales. The methodological contribution is a decision-oriented, seasonality-aware diagnostic workflow showing that shortage-relevant deficit frequency and wet-season timing uncertainty can intensify even when mean annual rainfall changes are small, offering a transferable template for other highly seasonal water-supply regions.

1 | Introduction

Understanding potential changes in precipitation under changing climate conditions is critically important for effective water resources management, agricultural planning, infrastructure resilience investment, and disaster risk reductions. Climate models project that global warming will alter precipitation patterns, intensifying the hydrological cycle and leading to spatially heterogeneous changes in rainfall distribution (IPCC 2021; Allan et al. 2020; Pendergrass et al. 2017) even at a regional scale. Increases in extreme precipitation events and longer dry spells have already been observed in many regions, posing threats to both flood risks and drought frequency (Hirabayashi et al. 2013; Fischer and Knutti 2016; Westra et al. 2014). Shifts in precipitation regimes can severely impact food security (Lobell et al. 2011), exacerbate water scarcity (Schewe et al. 2014),

and undermine existing ecological systems (Piao et al. 2010). Moreover, changing precipitation variability complicates the reliability of traditional hydrological design standards (Milly et al. 2008) and calls for adaptive management frameworks (Kundzewicz et al. 2007; Haasnoot et al. 2024). Regional disparities are particularly concerning, with some areas experiencing substantial increases while others face declines (Polade et al. 2017; Tebaldi et al. 2006). The interplay between temperature-driven evaporation and precipitation shifts also influences groundwater recharge and surface water sustainability which communities rely on (Asadieh and Krakauer 2015; Jones et al. 2024; Jung 2025). Reliable projections of precipitation under different warming scenarios thus form the foundation for climate adaptation policies (Swain et al. 2018).

Recent advancements in the Coupled Model Intercomparison Project Phase 6 (CMIP6) have significantly improved the simulation of hydrological processes at regional and local scales compared to earlier generations such as CMIP5. CMIP6 models feature enhanced spatial resolution, improved representation of land-atmosphere interactions, and more sophisticated physical parameterizations, leading to better capture of precipitation extremes, runoff variability, and soil moisture dynamics at finer spatial scales (Eyring et al. 2016; Ukkola et al. 2020; Zhang et al. 2025). Improvements in land surface schemes, such as more accurate modelling of evapotranspiration, snow processes, and groundwater exchanges, have enhanced the models' capability to simulate regional hydrological cycles (Lawrence et al. 2019; Swart et al. 2019). Moreover, CMIP6 models incorporate updated forcings, including Shared Socioeconomic Pathways (SSPs) and aerosol emissions, which allow for more realistic simulation of future climate and hydrological responses (O'Neill et al. 2016; Riahi et al. 2017). One of the main factors is the higher horizontal resolution (typically 1° or finer) reduces biases in orographic precipitation and river basin hydrology (Haarsma et al. 2016). As a result, using enhanced outputs from CMIP6 models, hydrological models can better present observed trends in hydrological extremes, such as floods and droughts, across diverse climatic zones (Li et al. 2022). These advancements provide a stronger basis for regional water resources planning and climate change adaptation efforts.

This study focuses on the Florida Peninsula, located in the southeastern United States. It has a unique hydroclimatic system characterised by its peninsular location, flat topography, extensive wetlands, and groundwater-dependent ecosystems (Marella 2008). Climate change has the potential to exacerbate existing challenges in water resources management, such as sea-level rise, saltwater intrusion, and changes in precipitation patterns (Obeysekera et al. 2017) in the region. Although there are few studies focusing on the Florida region, Srivastava et al. (2020) found that Multimodel medians of CMIP6 (CMIP6-MMM) and CMIP5 (CMIP5-MMM) have similar biases in climatology and variability but biases tend to be smaller in CMIP6-MMM. Zhao et al. (2023) found that CMIP6 ensemble median (CMIP6-EnM) can generally capture the observed extreme precipitation pattern. Wang and Asefa (2024) compared CMIP5 and CMIP6 climate models in simulating historical precipitation at the Florida Peninsula at multiple time scales and found that significant improvements in CMIP6 models were observed in capturing the rainy season in the Florida Peninsula, which accounts for about 60% of total annual rainfall and is driven by complex land-atmosphere–ocean interactions. None of the above-mentioned studies focused on potential changes in the characteristics of the rainy season, as well as drought risks related to cumulative rainfall deficit. This study aims to bridge the gap, and future discussions the implications for water resources management. The contribution of this study is therefore methodological and conceptual. We present a seasonality-aware, planning-relevant diagnostic framework that links bias-corrected CMIP6 ensembles to (i) variability metrics (monthly CV), (ii) a persistence-oriented drought proxy (12-month rolling, climatology-adjusted cumulative rainfall deficit, RCD), and (iii) rainy-season onset/demise behaviour.

The Remainder of This Paper Is Arranged as Follows. This Section Provides the Background and Motivation of the Study, Followed by a Description of Study Area and Methodology Section 2. In Section 3, Potential Changes in Rainfall Characteristics for Both the SSP-2.45 and SSP3-7.0 Scenarios Are Provided and Discussed. Concluding Remarks Are Provided in Section 4.

2 | Dataset and Methodology

2.1 | Historical and CMIP6 Dataset

The North American Land Data Assimilation System (NLDAS) provides high-resolution, gridded land surface datasets that integrate model simulations with observed atmospheric forcing to generate consistent, spatially continuous estimates of hydrological and land surface variables. Developed through collaboration between NASA, NOAA, and other institutions, NLDAS is designed to support research and applications related to water resources, drought monitoring, hydrological forecasting, and climate variability studies over the continental United States (Mitchell et al. 2004; Xia et al. 2012). NLDAS data are available at a spatial resolution of 1/8° (~12 km) and at hourly to monthly temporal scales, offering a long-term continuous record starting from the late 1970s. Key variables include precipitation, evapotranspiration, soil moisture, runoff, and temperature, among others. The high temporal and spatial resolution, combined with the consistent assimilation methodology, makes NLDAS particularly valuable for validating climate model outputs, analysing extreme hydrological events, and assessing changes in regional water availability. In this study, NLDAS precipitation from 1981 to 2010 in the Florida region were downloaded (https://hydro1.gesdisc.eosdis.nasa.gov/data/NLDAS/NLDAS_FORA0125_H.2.0/) and remapped to 1 degree longitude by 1 degree latitude spatial resolution.

Daily precipitation simulations from 18 CMIP6 General Circulation Models (GCMs) were obtained from the Earth System Grid Federation (ESGF) archives (https://esgf-node.llnl.gov/search/cmip6/) for the historical period 1981–2010. Corresponding future simulation data from the same set of GCMs were also collected. Although the period 1991–2020 is commonly used as a climatological baseline, many CMIP6 GCMs only extended their historical simulations to the mid-2010s. Therefore, 1981–2010 was selected as the climatology period for this study. The spatial resolution and modelling institution associated with each GCM are summarised in Table 1.

TABLE 1 | An overview of the model resolutions and the institutions that developed the various General Circulation Models (GCMs) in CMIP6, which are utilised in this study.

GCMS	Institute (Country)	Resolution
ACCESS-CM2	Commonwealth Scientific and Industrial Research Organisation (CSIRO) and the Australian Bureau of Meteorology (Australia)	1.25 degrees latitude ×1.875 degrees longitude
ACCESS-ESM1-5		1.875 degrees latitude ×1.875 degrees longitude
AWI-CM-1-1-MR	Alfred Wegener Institute (AWI) (Germany)	1 degree latitude ×1 degree longitude
BCC-CSM2-MR	Beijing Climate Center (BCC) (China)	1.125 degrees latitude ×1.125 degrees longitude
CNRM-CM6-1	Centre National de Recherches Météorologiques (CNRM) (France)	1.4 degrees latitude ×1.4 degrees longitude
CNRM-ESM2-1		1.4 degrees latitude ×1.4 degrees longitude
EC-Earth3-Veg-LR	European Centre for Medium-Range Weather Forecasts (ECMWF) (European Union)	2 degrees latitude ×2 degrees longitude
FGOALS-g3	Chinese Academy of Sciences (CAS) (European Union)	2 degrees latitude ×2.5 degrees longitude
GFDL-ESM4	Geophysical Fluid Dynamics Laboratory (GFDL) (United States)	2.5 degrees latitude ×2 degrees longitude
INM-CM4-8	Institute for Numerical Mathematics of the Russian Academy of Sciences (INM) (Russia)	2 degrees latitude ×2 degrees longitude
INM-CM5-0		1 degree latitude ×1 degree longitude
IPSL-CM6A-LR	Institut Pierre Simon Laplace (IPSL) (France)	1.9 degrees latitude ×2.5 degrees longitude
MIROC6	Japan Agency for Marine-Earth Science and Technology (JAMSTEC), National Institute for Environmental Studies (NIES), and Japan Atomic Energy Agency (JAEA) (Japan)	1.4 degrees latitude ×2.8 degrees longitude
MPI-ESM1-2-HR	Max Planck Institute for Meteorology (MPI-M) (Germany)	0.5 degrees latitude ×0.5 degrees longitude
MPI-ESM1-LR		1.9 degrees latitude ×1.9 degrees longitude
MRI-ESM2-0	Meteorological Research Institute (MRI) (Japan)	1 degree latitude ×1 degree longitude
NorESM2-LM	Norwegian Climate Prediction Model (NorCPM) and Norwegian Earth System Model (NorESM) (Norway)	1.875 degrees latitude ×2.5 degrees longitude
NorESM2-MM		1 degree latitude ×1 degree longitude

In this study, only the SSP-2.45 and SSP3-7.0 scenarios were selected for analysis. The SSP2-4.5 represents a "medium stabilisation" pathway, where moderate climate mitigation efforts lead to a stabilisation of radiative forcing by the end of the 21st century, making it comparable to the earlier RCP4.5 scenario and widely used for assessing plausible near- to mid-century climate risks (O'Neill et al. 2016). The SSP3-7.0 scenario, on the other hand, represents a "high forcing" pathway characterised by limited climate policy intervention and relatively high greenhouse gas emissions, corresponding to a radiative forcing of approximately 7.0 W/m^2 by 2100. Including SSP370 allows examination of more adverse climate futures and provides insights into the potential impacts under insufficient mitigation. Together, SSP245 and SSP370 span a broad range of possible future socio-economic and emissions trajectories without considering extreme scenarios (such as SSP1-2.6 or SSP5-8.5), making them particularly suitable for evaluating near-future and mid-century water resource planning.

Focusing on these two pathways strikes a balance between scientific comprehensiveness and practical relevance, especially for studies aimed at supporting adaptation and resilience strategies under uncertainty.

For all three datasets, including the daily precipitation from CMIP6 historical simulations, CMIP6 future simulations, and NLDAS observations, the Climate Data Operators (CDO) tool was used to remap the data to a uniform spatial resolution of 1° latitude by 1° longitude. CDO is an open-source, command-line software suite offering a wide range of functions, including file format conversion, data extraction, arithmetic operations, statistical computations, and basic visualisation (Schulzweida 2022). Using CDO, all precipitation datasets were standardised to the 1°×1° grid resolution, enabling consistent spatial analysis across data sources. The resulting datasets include historical GCM simulations for 1981–2010, corresponding NLDAS data, future projections for 2026–2055 and 2056–2085. Within the Florida Peninsula, this spatial resolution yields 24 grid cells, which were further aggregated into three geographic subregions: North Florida, Central Florida, and South Florida, as illustrated in Figure 1.

2.2 | Bias-Correction of Historical and Future Simulations From CMIP6 GCMs

To correct biases in the historical General Circulation Model (GCM) simulations, a quantile mapping technique was first applied. For each calendar month, the empirical cumulative distribution functions (CDFs) of the observed data and the GCM-simulated data were constructed. Each simulated data point was then bias-corrected by matching its cumulative probability to that of the observed data and assigning the corresponding observed value. Specifically, observed and simulated datasets were sorted independently for each month, and the quantile value of each simulated data point was mapped to the corresponding quantile of the observed dataset, that is, NLDAS dataset, as shown in Equation (1).

$$x_{m-r.adjst} = F_{o-c}^{-1}\left(F_{m-c}\left(x_{m-r}\right)\right) \tag{1}$$

where F is the CDF of either the observations (o) or model (m) for historic training or current period (c), retrospective runs (r), or for future projection period (p). In this method, for a given rainfall amount x_{m-r}, one first finds the percentile value of $F_{m-c}\left(x_{m-r}\right)$ using model CDF and then calculate the adjusted rainfall amount using the observed CDF, F_{o-c}^{-1}. Once this step is finished the bias corrected GCM CDF will match exactly that of the observed. This process adjusted not only the mean but also the variability and distributional characteristics of the GCM simulations to better align with observed climatology, thereby improving the fidelity of the historical baseline against which future changes are assessed (e.g., Teutschbein and Seibert 2012).

Following the historical data bias correction, a subsequent adjustment was applied to the raw future GCM projections. For each future simulation value, retrospective historical simulations within the same calendar month were used as a reference pool. As shown in Equation (2), for a given future percentile value of the projected data, the difference between the raw and bias-corrected retrospective data at that point was calculated. This difference served as the correction factor and was subtracted from the future raw simulation to obtain the final bias-corrected future projection as shown in equation below (Li et al. 2010). In short, for a p% future precipitation projection, x_{m-p}, the adjustment (error) obtained from CDF matching between observation and GCM retrospective model run is used as an adjustment for that percentile (Asefa and Adams 2013).

$$x_{m-p.adjst} = x_{m-p} + F_{o-c}^{-1}\left(F_{m-p}\left(x_{m-p}\right)\right) - F_{m-c}^{-1}\left(F_{m-p}\left(x_{m-p}\right)\right) \tag{2}$$

Additionally, corrected values smaller than 0.1 mm were set to zero to maintain physical plausibility. This two-step procedure ensures that both historical and future GCM outputs are adjusted to reflect observed statistics more accurately, while preserving the internal variability and trends essential for impact analysis. Figure 2 displays different datasets and processes in deriving the bias-corrected simulations for future years.

2.3 | Changes in Monthly and Annual Precipitation

The combination of outputs from the 18 GCMs is used to form a CMIP6 ensemble mean with equal weight to each GCMs. Ensemble averaging can also be obtained through GCMs weighting strategy based on certain performance criteria of individual models (Asefa and Adams 2013). But here it was left to be a simple arithmetic mean. The ensemble mean is treated as a separate model output in the evaluation described below. Therefore, there are, in total, 19 models used in results evaluation.

To evaluate the potential changes in the long-term average of annual precipitation under future climate scenarios, historical daily rainfall data from 1981 to 2010 is used as the baseline reference period. Future precipitation projections are derived from 18 General Circulation Models (GCMs) participating in CMIP6 for two distinct future periods: 2026–2055 and 2056–2085, under the two Shared Socioeconomic Pathways (SSPs). For each GCM and scenario, the average annual precipitation is calculated over the respective 30-year periods. The relative change in long-term average annual precipitation is then assessed by comparing the future projections to the historical baseline using Equation (3).

$$\Delta P_{i,s,t} = \overline{P}_{i,s,t} - \overline{P}_{hist} \tag{3}$$

where $\Delta P_{i,s,t}$ is change in mean annual precipitation for GCM i, scenario s, and time period t; $\overline{P}_{i,s,t}$ is the mean annual precipitation for GCM i, scenario s, and time period t; $\overline{P}_{hist}$ is the mean annual precipitation over the historical baseline period (1981–2010). There are two time periods, namely 2040s ($t=1$) and 2070s ($t=2$).

In addition to annual mean trends, long-term changes in monthly climatology are assessed to capture seasonal shifts in precipitation patterns under future climate scenarios. To further investigate changes in precipitation variability, the coefficient of variation (CV) of monthly rainfall is calculated for each period and scenario. The historical CVs (1981–2010) are then compared with those from the future periods (2026–2055 and 2056–2085) under SSP2-4.5 and SSP3-7.0.

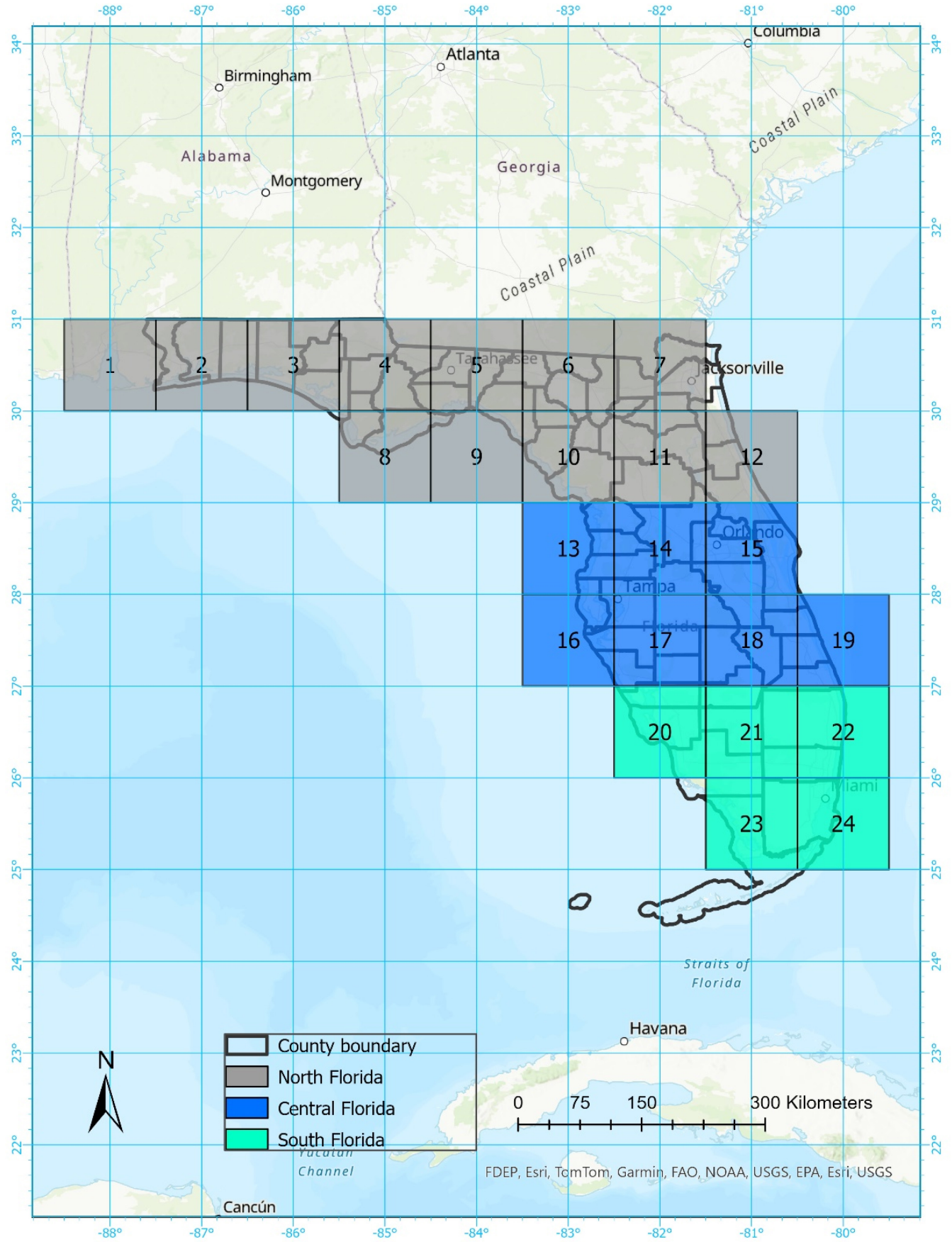

FIGURE 1 | Spatial layout of 1° × 1° grid boxes across the Florida Peninsula, labelled with grid IDs and grouped into North (1–12), Central (13–19), and South Florida (20–24). County boundaries are shown for reference. [Colour figure can be viewed at wileyonlinelibrary.com]

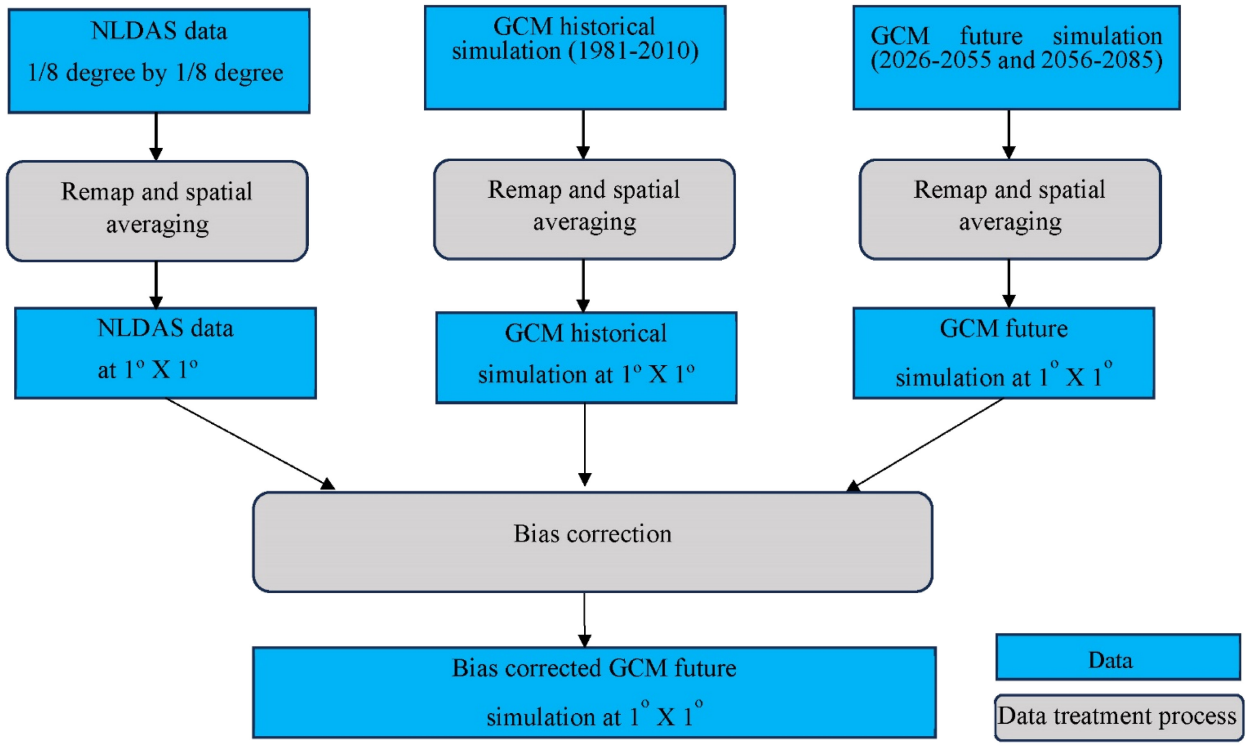

FIGURE 2 | Workflow for bias-correcting GCM precipitation using NLDAS data, covering historical (1981–2010) and future periods (2040s and 2070s). All data are remapped to 1°×1° resolution before bias correction. [Colour figure can be viewed at wileyonlinelibrary.com]

2.4 | Drought Indicator and Rainy Season Characteristics

To assess potential drought conditions triggered by prolonged rainfall deficits, this study employs the 12-month rolling cumulative rainfall deficit (RCD-rainfall) indicator. This metric, though not universally adopted, is used by regional water supply agencies in the Florida Peninsula to support water shortage assessments and planning. The RCD-rainfall indicator quantifies the cumulative deviation of monthly precipitation from its corresponding long-term monthly climatological mean, thereby capturing seasonally adjusted deficits.

Here, water shortage is defined in a supply-side sense using the precipitation-based RCD metric, representing cumulative deficits in rainfall inputs that can reduce hydrologic replenishment and constrain surface-water availability. Because RCD does not account for temperature-driven evaporative demand, the results should be interpreted as changes in precipitation-deficit hazard rather than a complete assessment of drought risk or total water-stress conditions under warming.

The RCD-rainfall for a given month t is computed as the sum of rainfall anomalies over the preceding 12 months, with each anomaly calculated relative to its respective calendar month's climatological average, as shown in Equation (4) below:

$$RCD_t = \sum_{k=t-11}^{t} \left(P_k - \overline{P}_{clim,m_k}\right) \tag{4}$$

where RCD_t is the 12-month rolling rainfall deficit at month t; P_k is the observed or simulated precipitation in month k; $\overline{P}_{clim,m_k}$ is the monthly climatological mean for the month m_k corresponding to time k, calculated over the corresponding 30-year period of interest. Note that the summation spans the 12 months ending in the month t.

To evaluate the frequency of potentially critical drought conditions, the percentage of months in which the RCD-rainfall indicator falls below a specified threshold θ (e.g., −127 mm or 5 in.) is calculated as shown in Equation (5). In this study, θ is set to −127 mm (−5 in), consistent with a cumulative rainfall-deficit trigger used by local water-supply agencies in the Florida Peninsula for shortage awareness and planning. This value is not intended as a universal standard; when applying the framework elsewhere, θ should be defined based on local operational drought triggers/planning criteria

$$Pct_{RCD<\theta} = \frac{1}{N}\sum_{t=12}^{T} I\left(RCD_t < \theta\right) \times 100\,\% \tag{5}$$

where T is the total number of months in the 30-year period (i.e., 360); N is the number of months for which the RCD can be calculated and is 11 less than T as the first 11 months lack a complete 12-month window; $I(\cdot)$ is the indicator function equal to 1 if the condition is true and 0 otherwise. The RCD effectively represents the drought as it relates to climatic drivers (in this case only rainfall is considered).

This percentage is computed, for each grid box, for the historical baseline period (1981–2010) and for the future periods

(2026–2055 and 2056–2085), across multiple General Circulation Models (GCMs) and two SSP scenarios (SSP2-4.5 and SSP3-7.0). The comparison across periods enables an assessment of how the frequency of extended rainfall deficits may evolve under changing climatic conditions.

A distinguishing feature of the evaluation is that the drought/shortage proxy is formulated to be explicitly seasonality-adjusted. Because the climatological mean differs substantially by calendar month in highly seasonal regimes, the RCD metric accumulates monthly anomalies relative to each month's climatology (rather than accumulating raw departures from an annual mean). This preserves the physical meaning of "deficit persistence" across wet and dry seasons and avoids conflating normal dry-season conditions with drought.

Another important characteristic of rainfall in the Florida Peninsula is the behavior of the rainy season, as regional water supply agencies rely on wet-season precipitation to replenish within-year reservoir fillings and uses (during the dry months). Potential changes in key rainy season attributes, such as onset and demise dates, total rainfall accumulation, and interannual variability, could significantly affect water availability and the operational reliability of water supply systems. Although the summer months of June through September (JJAS) generally comprise the core of the rainy season, its exact onset and demise cannot be precisely defined by the beginning or end of calendar months due to substantial year-to-year variability. The method used to determine the onset and demise of the rainy season is omitted here for brevity; readers are referred to previous studies for methodological details (Misra and DiNapoli 2013; Misra et al. 2018; Wang and Asefa 2024). In essence, the onset date of the summer season for a region of interest is defined as the date that reaches the minimum in the daily cumulative anomaly curve. The demise of the summer season is defined as the date that has the maximum in the daily cumulative anomaly curve. In this study, characteristics of the rainy season are first evaluated for the historical baseline period (1981–2010) and subsequently analyzed for future conditions using simulations from multiple GCMs under two Shared Socioeconomic Pathways (SSP2-4.5 and SSP3-7.0) across two 30-year projection windows: 2026–2055 and 2056–2085.

3 | Results and Discussion

Figure 3a shows the boxplots of estimated changes of annual precipitation at different grid boxes for the two future time periods, based on the SSP2-4.5 scenario. Figure 3b shows similar information based on the SSP3-7.0 scenario. Under SSP2-4.5, projected changes in annual precipitation across the Florida Peninsula exhibit a spatial gradient, with larger increases in northern regions and smaller or even negative changes in the south. Using simulations from 18 GCMs and their multi-model mean (19 models total), results show that for the near-future period (2026–2055), most grid boxes experience increases ranging from approximately 2–9 in. annually, with mean changes generally higher in northern Florida (grid boxes 1–12) and tapering southward. For the late-century period (2056–2085), this increasing trend persists and intensifies in many locations, particularly in northern and central Florida, while southern Florida (grid boxes 20–24) shows more modest gains or near-zero changes. These results suggest a gradual wetting trend in the northern part of the state under a moderate emissions scenario, which may provide potential benefits for water resource availability if effectively managed. Note that since most climate projections show an increase in temperature (not shown here), whether there is a net usable benefit of increased rainfall translates into surface water or groundwater depends on several factors, including intra- and inter-annual distribution and hydrologic conditions. This requires verification through integrated hydrologic modelling (Chang et al. 2018), which is beyond the scope of the current study.

Under SSP3-7.0, projected changes in annual precipitation show a similar spatial pattern but with enhanced variability and more pronounced decreases in southern Florida. The near-future period (2026–2055) shows moderate increases (2–7 in. annually) in the northern and central parts of the state, with more muted or negative changes appearing in the southern grid boxes. In the late-century projections (2056–2085), northern and central Florida maintain positive trends in annual precipitation, but grid box #23 shows a decrease of 1.5 in. at the 50th percentile for the 2070s. This divergent pattern indicates a heightened risk of long-term drying in southern Florida under a higher emissions scenario, which could intensify water scarcity challenges in a region already vulnerable to seasonal variability and saltwater intrusion.

Projected changes in monthly precipitation climatology, as depicted in Figure 4, reveal notable spatial and seasonal variability across the Florida Peninsula. Grid boxes #3 (north), #11 and #13 (central), and #21 (south) are selected to represent distinct hydroclimatic regions. For northern Florida (grid #3), projections indicate consistent increases in monthly precipitation during the summer months (June–September), with changes reaching up to 1.5 in., especially by the late-century period (2056–2085). Central Florida (grids #11 and #13) shows more mixed patterns: while summer months generally exhibit modest decreases, several months—particularly during spring and early winter—display slight increases or limited change. In contrast, southern Florida (grid #21) exhibits the highest month-to-month variability, with alternating signals of both increases and decreases depending on the month and time period. Overall, while summer wet-season intensification is evident in the north, more uncertain and variable patterns emerge in the central and southern regions, underscoring the importance of region-specific planning in adapting to future hydroclimatic shifts.

Under SSP3-7.0, as shown in Figure 5, projected changes in monthly precipitation climatology across Florida show similar seasonal structures to SSP2-4.5 but with amplified variability and a greater likelihood of monthly deficits, particularly in central and southern regions. In northern Florida (grid #3), most months show increased precipitation, especially during the summer wet season (June–September), with projected gains of up to 1.5 in. by the late-century period (2056–2085). However, the variability across models is slightly greater than under SSP2-4.5. Central Florida (grid boxes #11 and #13) exhibits more mixed signals: grid #11 continues to show modest increases in many months, but grid #13 reveals pronounced reductions during the summer (June–August), with projected

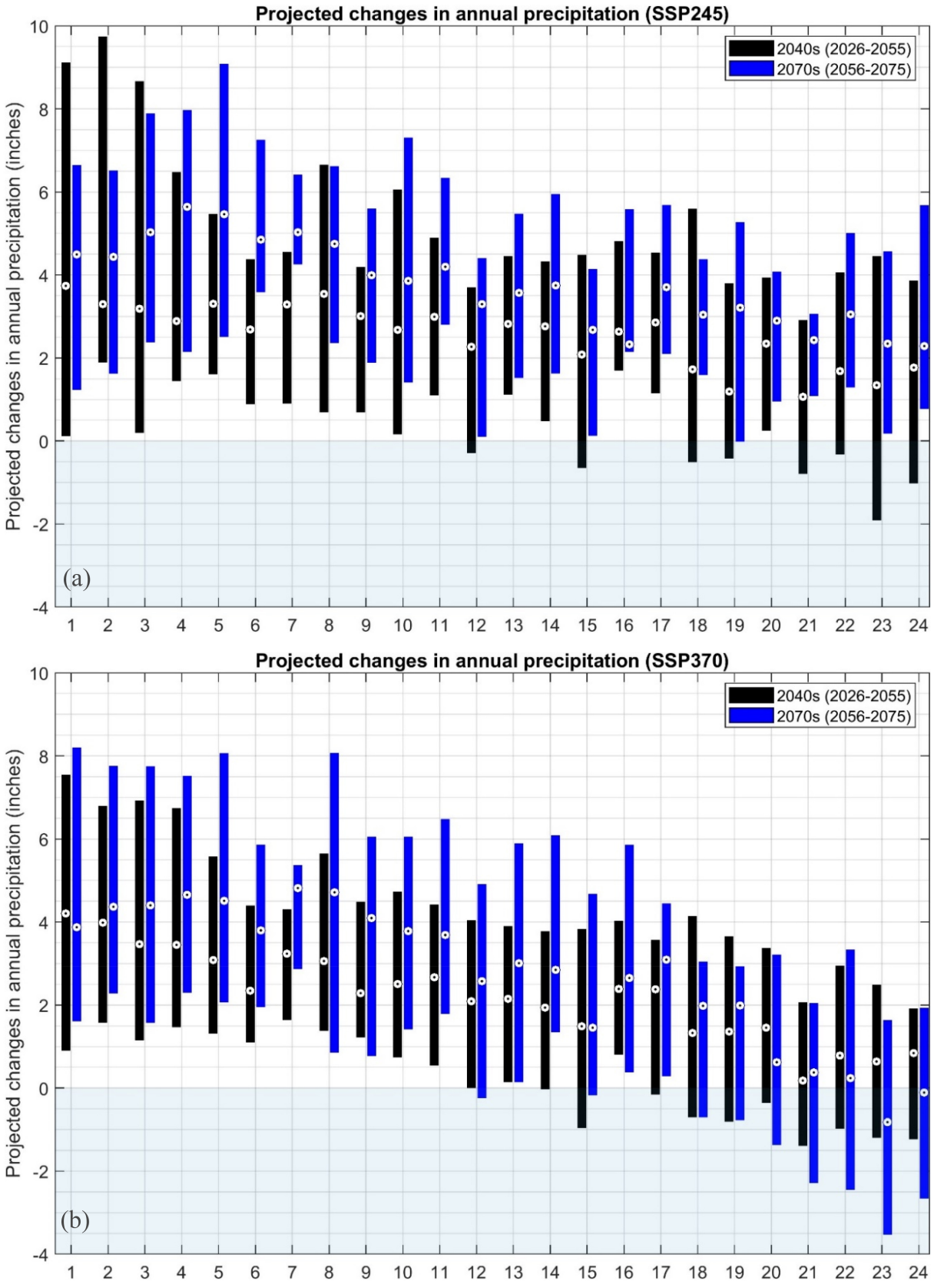

FIGURE 3 | Projected changes in annual precipitation across 24 grid boxes for the 2040s and 2070s under (a) SSP2-4.5 and (b) SSP3-7.0. Bars show model ranges; circles indicate multi-model ensemble means. The shaded area represents when values are negative, indicating drier futures. [Colour figure can be viewed at wileyonlinelibrary.com]

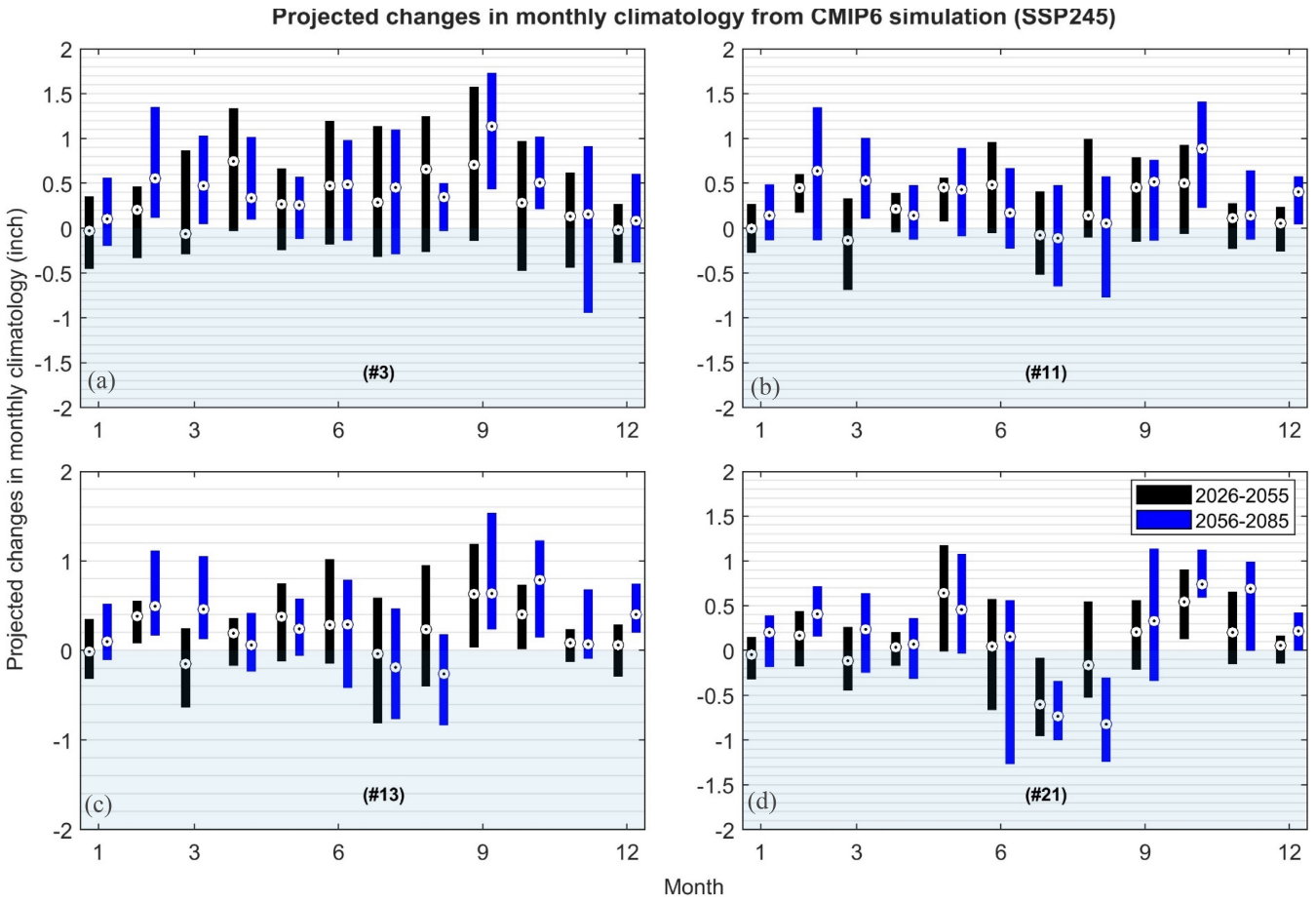

FIGURE 4 | Monthly precipitation changes under SSP2-4.5 for four selected grid boxes. Black and blue bars show projections for the 2040s and 2070s, respectively. Shaded areas represent when the values are negative, indicating potential drying. [Colour figure can be viewed at wileyonlinelibrary.com]

declines approaching −1 in. per month by the late century. Southern Florida (grid #21) shows the most significant declines, particularly in the early to mid-summer months, with several ensemble means dipping below zero. This drying signal, coupled with higher emissions and warming, could exacerbate hydrologic stress in an already climate-sensitive region. Overall, SSP3-7.0 projections suggest an elevated risk of reduced seasonal predictability and increasing month-to-month extremes, which could complicate reservoir management and water supply reliability across the state.

Southern Florida rainfall is strongly shaped by the seasonal migration of the convective rain belt and by circulation over the Gulf of Mexico–Caribbean–western Atlantic region. While this study does not explicitly diagnose circulation or moisture-transport fields, the projected drying signal in southern Florida under SSP3-7.0 is consistent with mechanisms discussed in prior work. In particular, shifts in the position/strength of the North Atlantic Subtropical High (Bermuda High/NASH) can alter low-level flow, subsidence, and moisture convergence over the Southeast, influencing warm-season rainfall organisation (Li et al. 2011; Nieto Ferreira and Rickenbach 2020). More broadly, greenhouse warming is linked to a poleward expansion of the Hadley circulation and subtropical dry zones, which can increase the frequency of subsidence-dominated regimes at subtropical latitudes (Lu et al. 2007; Seidel et al. 2008; Schmidt and Grise 2017). Finally, wet-season rainfall over Florida is sensitive to SST patterns and moisture supply from the Intra-Americas Seas; changes in regional SST gradients can modulate moisture transport and convective activity (Wang et al. 2008; Misra and DiNapoli 2013; Misra et al. 2018).

Projected changes in the coefficient of variation (CV) of monthly precipitation reveal a clear tendency toward increased rainfall variability across the Florida Peninsula under both SSP2-4.5 and SSP3-7.0 scenarios, as shown in Figure 6. Projected spatial trends across the state are consistent with historical observations. During the historical baseline period (1981–2010), CV values are generally lower in northern Florida (grid boxes 1–12), with most values ranging between 0.55 and 0.70, reflecting relatively stable month-to-month precipitation patterns. In contrast, central Florida (grid boxes 13–19) begins to show slightly higher CVs, while southern Florida (grid boxes 20–24) exhibits the highest baseline variability, with several CV values exceeding 0.75. This spatial gradient indicates an inherent increase in monthly rainfall variability from north to south during the reference period.

In the future projection periods (2026–2055 and 2056–2085), both scenarios show consistent increases in CV across most grid boxes, but the magnitude and extent of change vary by region. Under SSP2-4.5, northern Florida experiences modest CV

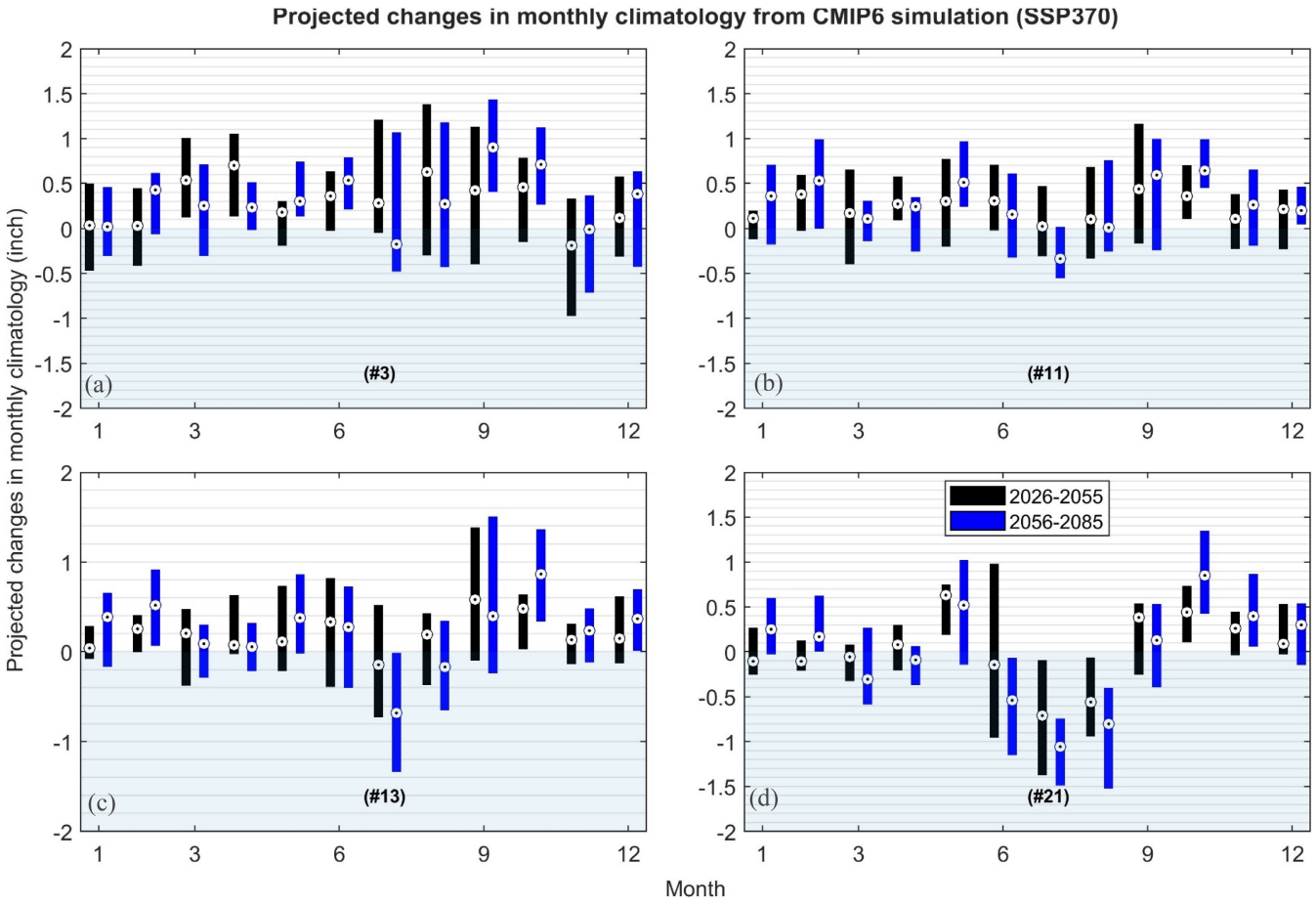

FIGURE 5 | Monthly precipitation changes under SSP3-7.0 for four selected grid boxes. Black and blue bars show projections for the 2040s and 2070s, respectively. Shaded areas represent when the values are negative, indicating potential drying. [Colour figure can be viewed at wileyonlinelibrary.com]

increases. Central Florida exhibits more noticeable increases, especially during the late-century period, while southern Florida shows the largest jumps, with several grid boxes exceeding 0.80 in CV by the 2070s—indicating a substantially more erratic monthly rainfall regime. Under SSP3-7.0, this pattern is amplified: CV values rise more sharply across all regions, and grid boxes in southern Florida show the greatest divergence from baseline conditions. This intensified variability, particularly in the southern part of the state, signals heightened risks for water management, as extreme dry or wet months may occur more frequently even if mean annual precipitation increases. A previous study found that increased precipitation variability leads to a growing decoupling between total rainfall and its hydrological utility. This divergence emerges from significant shifts in rainfall temporal structure that impact how effectively rainfall contributes to surface and subsurface water storage, crop water availability, and overall ecosystem functionality (Wang et al. 2026).

While intra- and interannual variability are important considerations, it is often persistent deficits that exacerbate multi-year shortages or surpluses—dynamics that critically influence both supply- and demand-side water management decisions. Given that most storage infrastructure in Florida functions on a within-year basis, assessing the consequence of persistent hydroclimatic regimes is essential. Figure 7 illustrates the evolution of the cumulative rainfall deficit (RCD) at grid box #13 (central Florida) based on simulations from the ACCESS-CM2 model under the SSP3-7.0 scenario. The plots compare three time periods: the historical baseline (1981–2010), near future (2026–2055), and far future (2056–2085). During the historical period, episodes of RCD falling below the critical threshold, which define management actions, are intermittent and relatively moderate in duration and intensity. The total percentage of time the RCD was below the threshold during this period was 27.22%, indicating that extreme cumulative rainfall deficits were relatively infrequent.

In contrast, the projected future periods show a clear intensification of rainfall deficits. From 2026 to 2055, the RCD falls below the threshold for 37.53% of the time, reflecting longer and more frequent drought events. This elevated frequency persists into the 2056–2085 period, where the RCD remains below the threshold for 35.53% of the months. These changes are not only evident in the increased duration of deficits but also in the depth of drought conditions, with several periods in the far-future simulation showing sustained RCD values below −20 in. The progressive increase in both the frequency and magnitude of cumulative rainfall deficits underlines a growing risk of prolonged hydrologic droughts.

After aggregating the information across multiple GCMs, Figure 8a,b depict the projected percentage of time that the

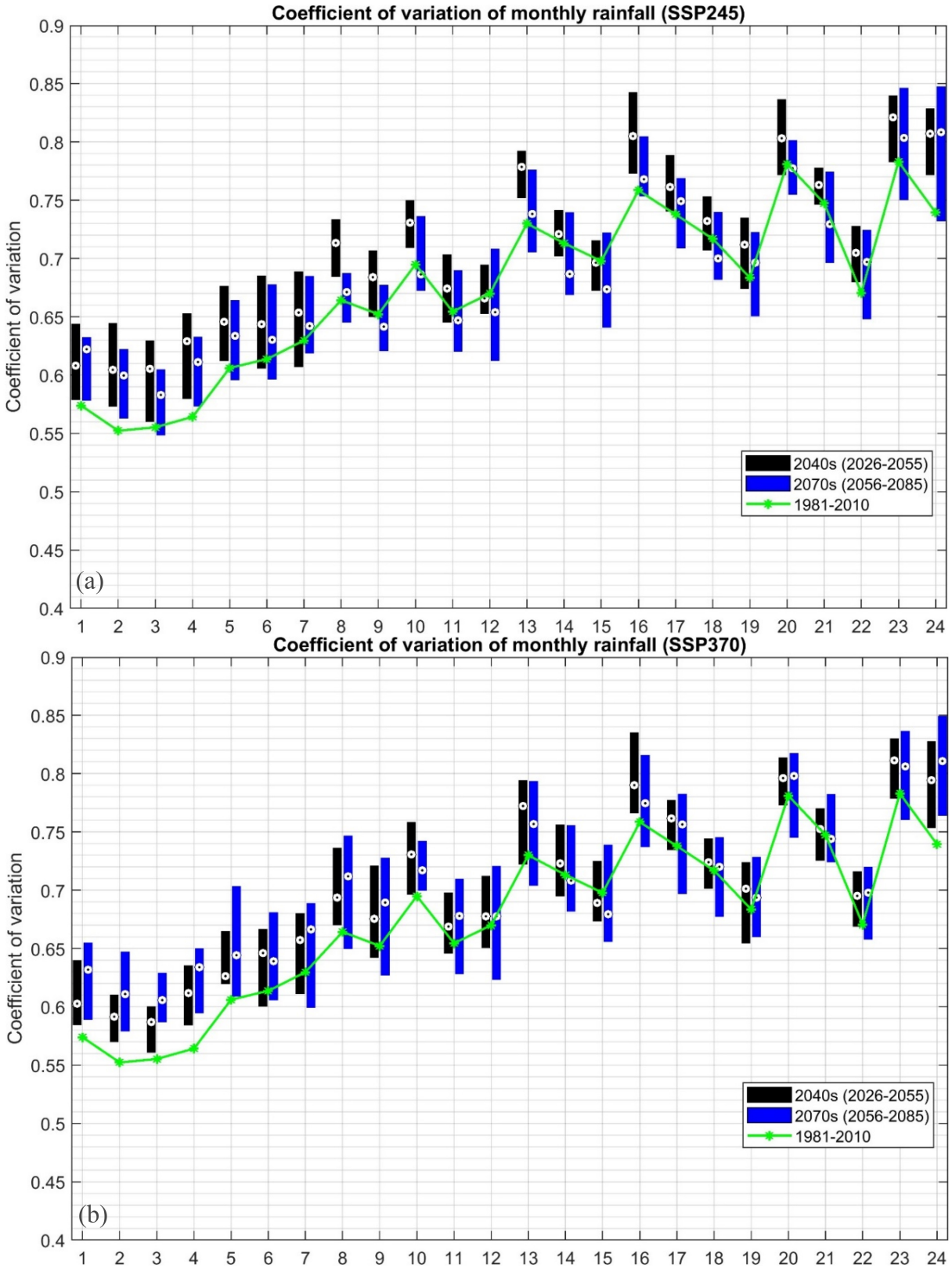

FIGURE 6 | Coefficient of variation (CV) of monthly rainfall for baseline, 2040s, and 2070s across grid boxes under (a) SSP2-4.5 and (b) SSP3-7.0. Increased CV suggests rising rainfall variability, especially under SSP3-7.0. [Colour figure can be viewed at wileyonlinelibrary.com]

cumulative rainfall deficit (RCD) falls below a pre-defined drought threshold, which serves as a proxy for potential water shortage conditions across the 24 spatial grid boxes in the Florida Peninsula. Results are shown for the baseline period (1981–2010) and two future periods (2026–2055 and 2056–2085) using 18 CMIP6 General Circulation Models (GCMs) and their ensemble mean (19 in total). Under SSP2-4.5 (Figure 8a), the baseline percentage of time below the threshold typically ranges between

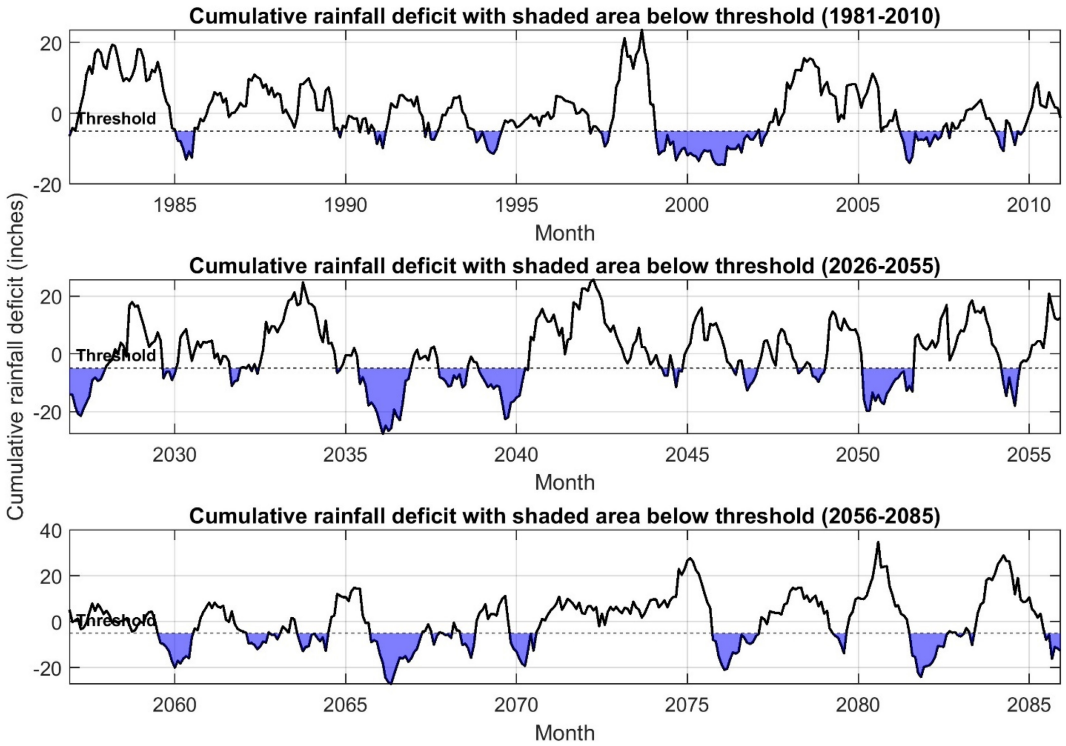

FIGURE 7 | Example of cumulative rainfall deficit (RCD) for grid #13 under SSP3-7.0. Shaded areas indicate drought periods when RCD falls below threshold during baseline and future periods. [Colour figure can be viewed at wileyonlinelibrary.com]

26% and 32% across most grid boxes. However, future projections indicate a consistent upward shift in drought frequency. For many northern and central grid boxes (e.g., 1–19), the mean projected percentage of time under water shortage increases to 34%–36% by mid-century and continues to rise slightly toward the late century. The increases are particularly prominent in northern Florida (grid boxes 1–12), where several models project values exceeding 36% by 2070s. In southern Florida (grid boxes 20–24), baseline drought frequency is already relatively high, and future projections suggest even greater vulnerability, with some ensemble values nearing or surpassing 38% of months under deficit conditions.

Under the higher-emission SSP3-7.0 scenario (Figure 8b), the increase in projected water shortage frequency is more pronounced across all regions. Northern Florida grid boxes show projected increases of 5–10 percentage points over baseline values, reaching up to 39%–40% of months by the 2070s. Central Florida grid boxes display similar trends, while southern Florida again emerges as a hotspot of drought vulnerability, with consistently higher-than-average percentages in both mid- and late-century periods. The spread among models also increases under SSP3-7.0, suggesting heightened uncertainty and variability in projected hydrologic stress. Overall, these results signal a robust trend toward more frequent and persistent drought-like conditions across Florida, especially under higher emissions scenarios, highlighting the importance of incorporating climate-informed indicators such as RCD into long-term water resource planning and drought preparedness strategies.

One limit associated with RCD is that it is based solely on precipitation. In a warming climate, increases in atmospheric evaporative demand can amplify hydroclimatic stress even if rainfall remains unchanged, because higher temperature, net radiation, and vapour pressure deficit can increase potential evapotranspiration (PET) and shift the surface water balance toward greater losses. As a result, precipitation-only drought and seasonality metrics may underestimate changes in effective water availability and drought risk, particularly during warm-season periods when evaporative demand is highest and soil moisture depletion can be rapid.

Three to four months of rainfall provide about 50%–60% of Florida's annual total, making summer season shifts especially significant. Figure 9 presents projected changes in rainy season precipitation for three regions across the Florida Peninsula—northern, central, and southern Florida—under the SSP2-4.5 scenario. Each subplot displays individual model outputs from 18 CMIP6 GCMs and one ensemble mean (CMIP6-Ensemble), with boxplots representing the 30-year distributions for two future periods: 2026–2055 (black) and 2056–2085 (blue). The dashed horizontal line in each panel indicates the historical average (1981–2010) for comparison.

In northern Florida, most models project future rainy season totals that are comparable to or slightly above the historical average of approximately 26 in. While inter-model variability is evident, particularly in the 2040s, the ensemble mean remains close to historical levels in both future periods, suggesting modest changes in average seasonal rainfall. Notably, a few models (e.g., MIROC6, GFDL-ESM4) show more pronounced increases in rainy season precipitation by the 2070s.

For central Florida, projected changes are more mixed. Several models predict a slight decrease in median rainy season precipitation, while others show minor increases. The ensemble average remains relatively stable across time periods, hovering near the historical reference (~30 in.). However, individual models

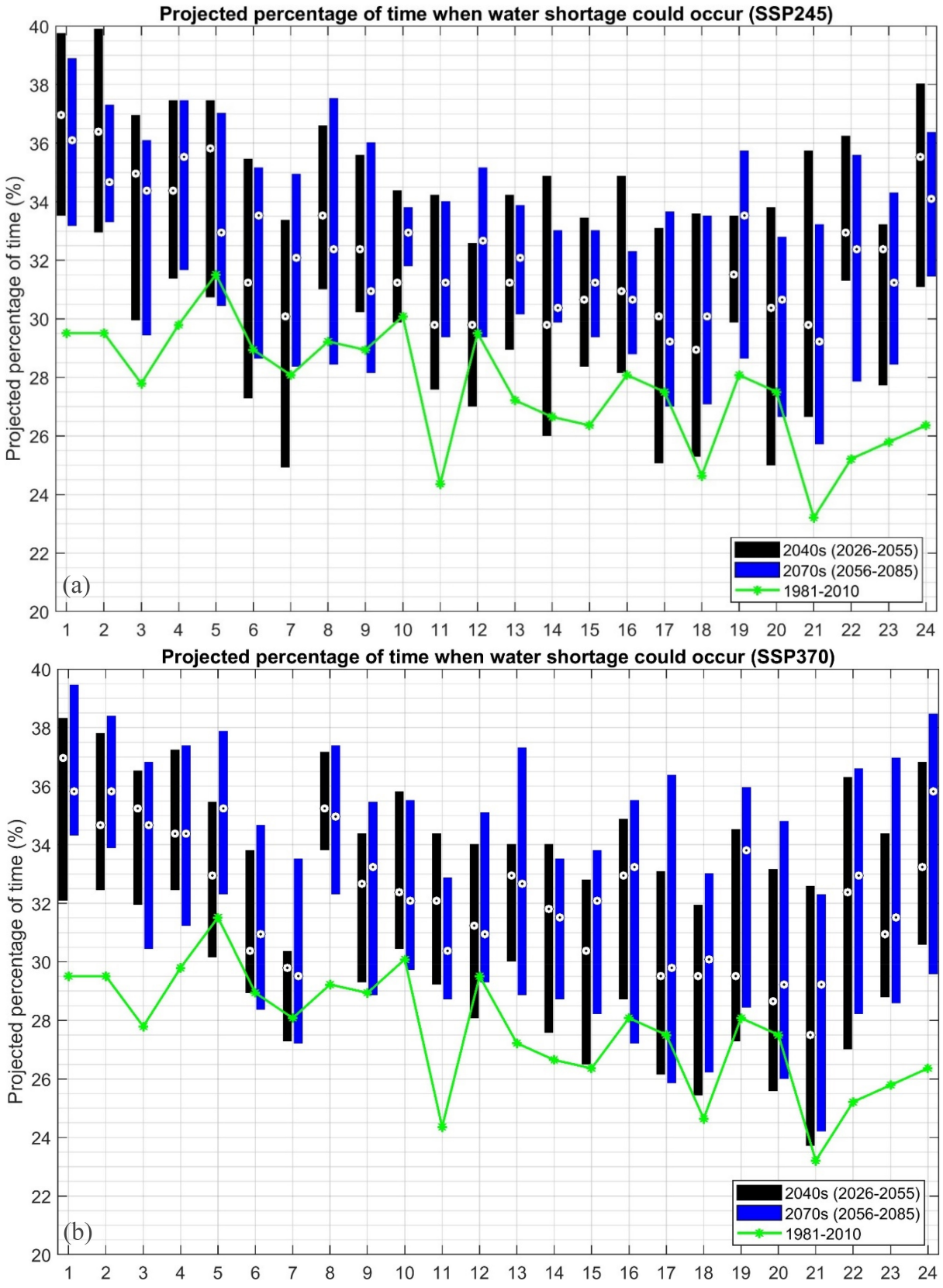

FIGURE 8 | Projected percentage of time RCD falls below the drought threshold across grid boxes for baseline, 2040s, and 2070s under (a) SSP2-4.5 and (b) SSP3-7.0. Future increases in drought frequency are evident. [Colour figure can be viewed at wileyonlinelibrary.com]

like INM-CM5-0 and MRI-ESM2-0 suggest potentially drier conditions during the late century, indicating localized risks despite overall ensemble stability.

In southern Florida, the historical rainy season rainfall is higher (~34 in.), and projections show a broader range of future outcomes. While a few models indicate increased precipitation (e.g.,

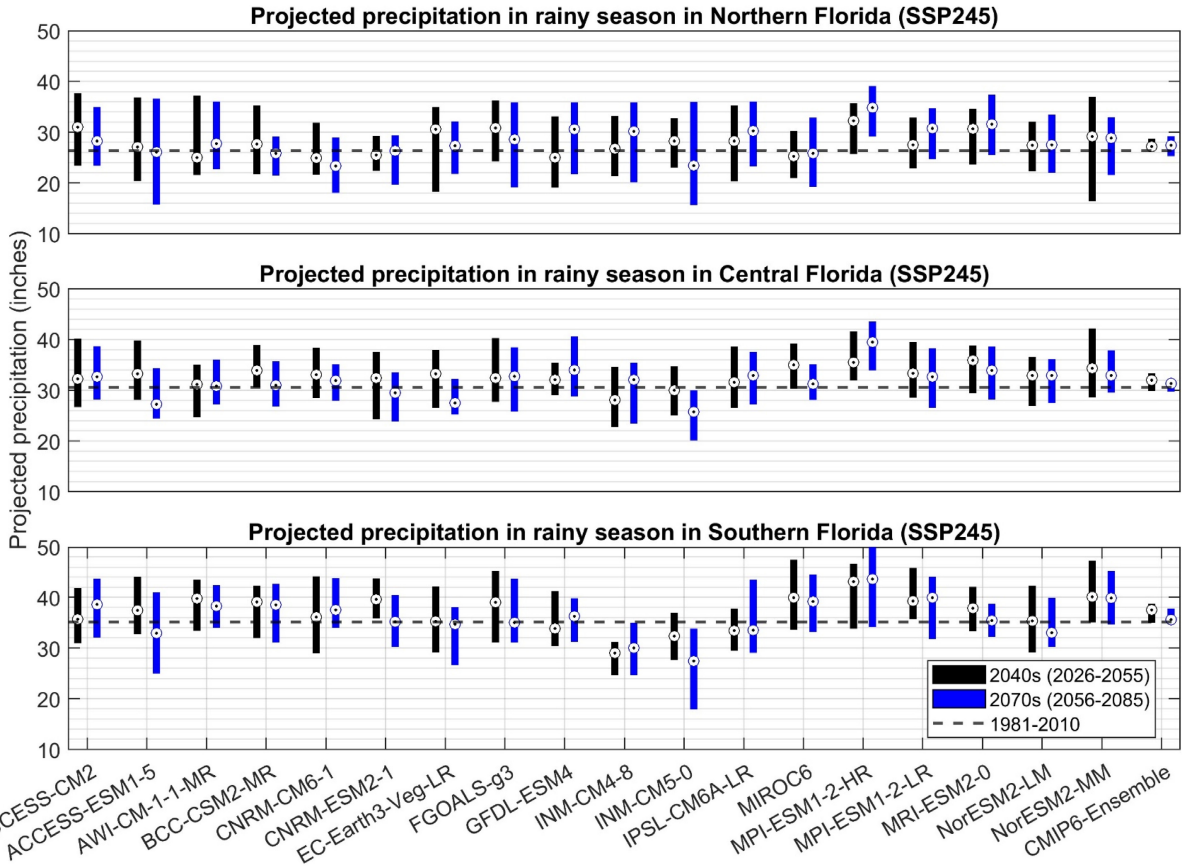

FIGURE 9 | Projected precipitation during the summer rainy season across Northern, Central, and Southern Florida under the SSP2-4.5 scenario. The figure compares future projections for two 30-year periods—2040s (2026–2055, black bars) and 2070s (2056–2085, blue bars)—with the baseline historical period (1981–2010, dashed line). The dashed line indicates the historical average, while circle markers denote ensemble means for future projections. [Colour figure can be viewed at wileyonlinelibrary.com]

MPI-ESM1-2-HR, MIROC6), others suggest noticeable reductions, especially in the 2040s. The ensemble mean remains generally consistent with the baseline, but the interquartile range slightly narrows by the 2070s, hinting at reduced interannual variability.

Figure 10 illustrates projected changes in rainy season precipitation across northern, central, and southern Florida under the SSP3-7.0 scenario. In northern Florida, projected changes exhibit considerable inter-model spread, with some GCMs suggesting increased seasonal precipitation and others indicating declines. Despite this variability, the ensemble mean remains relatively close to the historical baseline (approximately 26 in.) in both future periods. Notably, more models tend to predict above-average rainfall by the late century (2070s), though the range remains broad, reflecting heightened uncertainty under the higher-emission scenario.

Central Florida shows a similar pattern of variability, with most models projecting precipitation totals near or slightly above the historical average (~30 in.). However, a few models (e.g., INM-CM4-8, INM-CM5-0) indicate modest decreases in rainy season rainfall. The ensemble mean suggests stability across both future periods, though the presence of models projecting wetter and drier futures signals the need for flexible water management strategies.

In southern Florida, where the historical rainy season average is higher (~34 in.), the projected changes show somewhat greater consistency across models. Many GCMs suggest a slight increase or stability in rainy season totals by mid-century, while late-century projections under SSP3-7.0 indicate potential increases in precipitation for several models (e.g., MIROC6, MPI-ESM1-2-HR). The ensemble mean remains nearly unchanged between the historical baseline and future periods, suggesting that while individual model responses vary, the average seasonal rainfall may remain relatively robust in southern Florida under this scenario.

Overall, the SSP3-7.0 projections indicate that rainy season precipitation totals may remain broadly comparable to historical values across the Florida Peninsula, though model-level variability increases under this higher-emission scenario.

A comparison between the SSP2-4.5 and SSP3-7.0 scenarios reveals both commonalities and key differences in projected rainy season precipitation across the Florida Peninsula. Under both scenarios, the multi-model ensemble mean suggests relatively stable seasonal rainfall totals through mid- and late-century periods, with most deviations from the historical mean falling within a ±5 in. range. However, projections under SSP3-7.0 tend to show a wider inter-model spread, particularly in northern and central Florida, indicating greater uncertainty and the potential

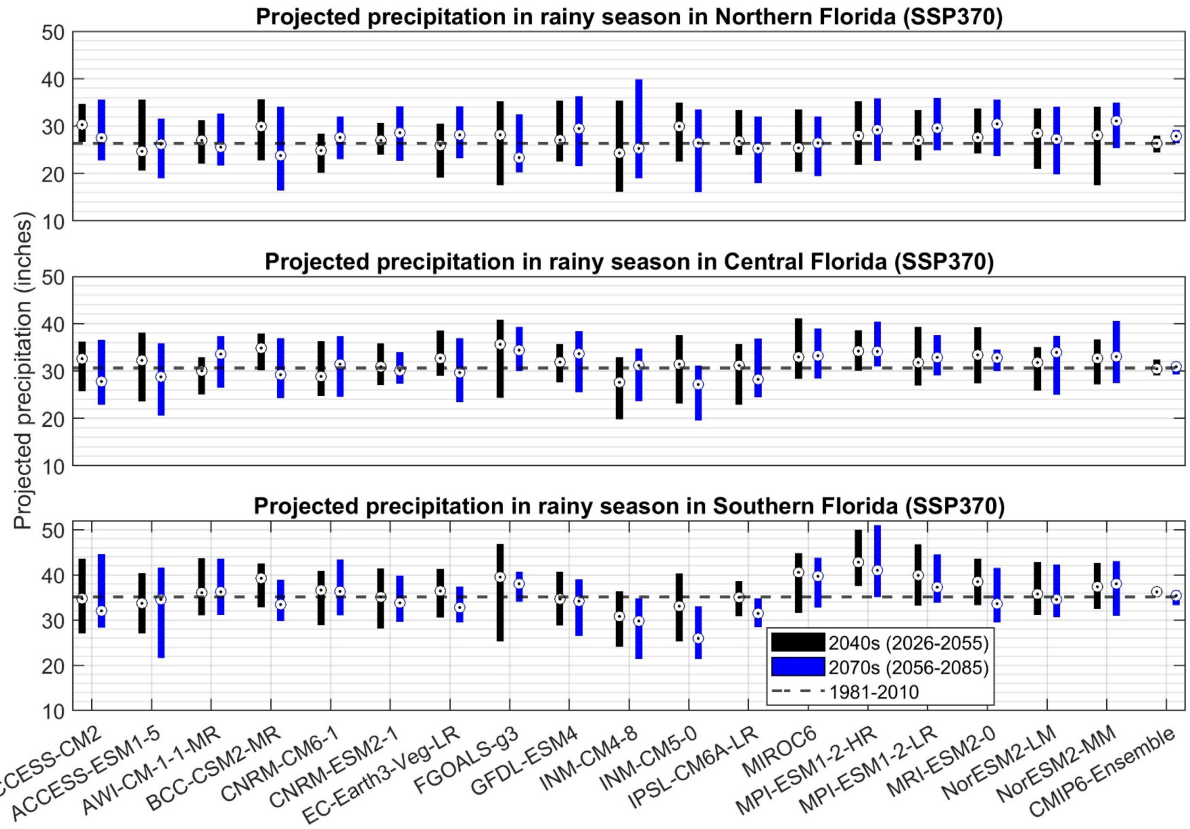

FIGURE 10 | Projected precipitation during the summer rainy season across Northern, Central, and Southern Florida under the SSP3-7.0 scenario. The figure compares future projections for two 30-year periods—2040s (2026–2055, black bars) and 2070s (2056–2085, blue bars)—with the baseline historical period (1981–2010, dashed line). The dashed line indicates the historical average, while circle markers denote ensemble means for future projections. [Colour figure can be viewed at wileyonlinelibrary.com]

for more pronounced changes under the higher-emission pathway. In contrast, SSP2-4.5 projections appear more constrained, with a majority of models clustering closely around the historical baseline. Notably, southern Florida demonstrates relatively consistent projections across both scenarios, with the ensemble mean remaining nearly unchanged and several models even suggesting slight increases in seasonal rainfall. These results suggest that while the overall magnitude of rainy season precipitation may remain comparable to historical levels, higher-emission scenarios such as SSP3-7.0 could introduce greater variability and risk, especially in the northern portions of the state. This underscores the importance of scenario-based planning to ensure resilient water supply systems across a range of possible future conditions.

Figure 11 presents the projected rainy season onset dates for Central Florida under two future time periods (2026–2055 and 2056–2085) and two emission scenarios (SSP2-4.5 and SSP3-7.0), based on outputs from the 19 CMIP6 global climate models (GCMs). The top row displays scatter plots of annual onset dates from each GCM, colour-coded relative to the historical climatological mean onset date (151 day-of-year): early (more than 7 days earlier; blue), within a ±7-day window (grey), and late (more than 7 days later; orange). The SSP2-4.5 scenario is plotted with fully opaque markers, while SSP3-7.0 uses semi-transparent markers to visually distinguish between scenarios. The bottom row shows the percentage distribution of these onset timing categories for each model.

Compared to the historical record, future projections reveal not only a tendency toward later onset dates, particularly under the high-emission SSP3-7.0 scenario and during the later period (2056–2085), but also a marked increase in interannual variability. This is evident from the wider vertical spread of onset dates across most models, especially under SSP3-7.0. Additionally, the percentage distribution of onset timing categories shows a notable shift: the proportion of years with onsets falling within the ±7-day climatological window decreases substantially, while the proportion of late onsets increases. Early onsets remain relatively rare in most models and scenarios. These combined changes, toward later, more variable, and less climatologically consistent onset dates, highlight growing challenges for water resource management in Central Florida under future climate conditions. Results for Northern Florida and Southern Florida are similar, and these are provided in Figures S1 and S2.

The framework is transferable because it is defined in terms of generic diagnostics (mean, variability, persistence, and seasonal timing) rather than Florida-specific hydrologic infrastructure. For other regions, the same workflow can be implemented with locally appropriate choices of (i) the deficit accumulation window (e.g., 6–24 months depending on storage memory), (ii) the deficit threshold tied to local drought triggers or planning criteria, and (iii) the definition of wet-season onset/demise suitable for the regional precipitation regime. The central conceptual message remains the same: annual precipitation statistics alone are insufficient to characterise climate stress on seasonal

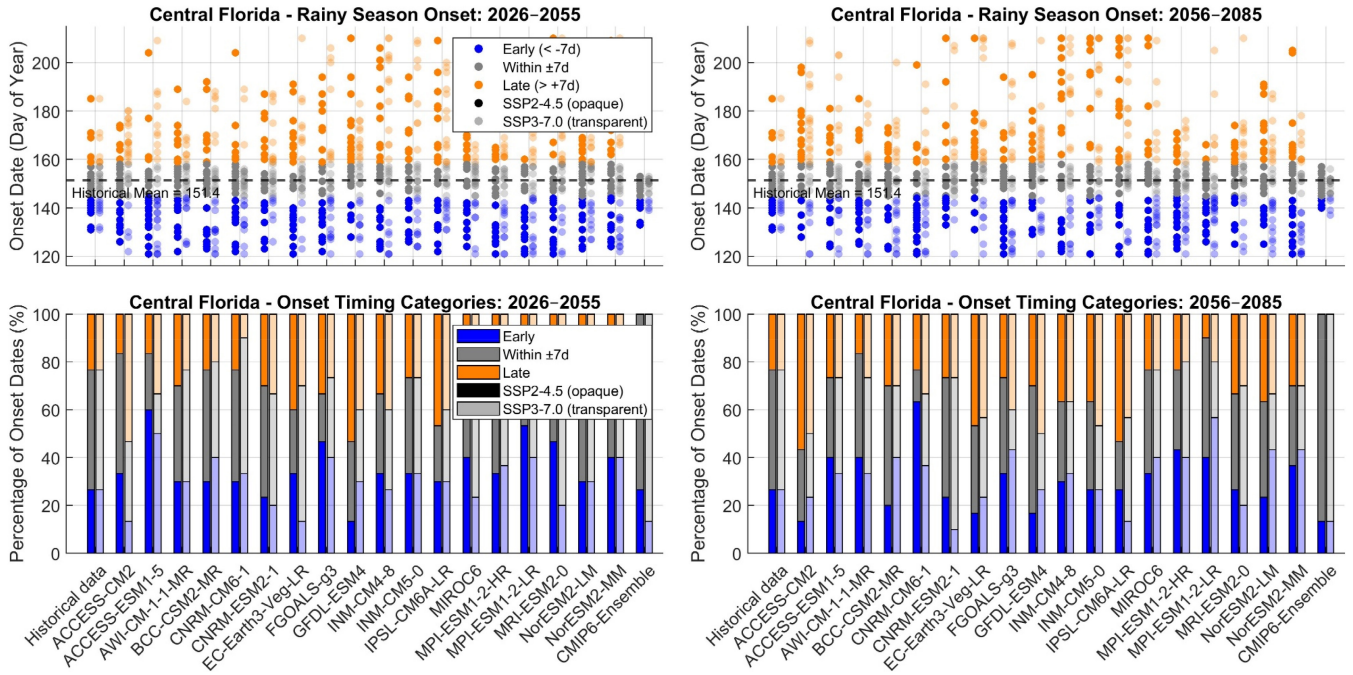

FIGURE 11 | Projected rainy season onset dates in Central Florida under two future periods (2026–2055 and 2056–2085) and two emission scenarios (SSP2-4.5 and SSP3-7.0) across 19 CMIP6 climate models. Top panels show rainy season onset dates by model, colour-coded as early (blue), within ±7 days of the historical mean (grey), or late (orange); transparency indicates scenario (opaque = SSP2-4.5, transparent = SSP3-7.0). Dashed line marks the historical mean onset (day 151.4). Bottom panels show the percentage of onset timing categories per model. Results highlight a shift toward later and more variable onset under higher emissions. [Colour figure can be viewed at wileyonlinelibrary.com]

water-supply reliability, which is controlled by the interaction of variability, persistence of deficits, and wet-season timing.

4 | Conclusion

This study assessed potential changes in precipitation characteristics across the Florida Peninsula using simulations from 18 CMIP6 General Circulation Models (GCMs) and their ensemble mean under two Shared Socioeconomic Pathways (SSP2-4.5 and SSP3-7.0). This study aims to evaluate changes in annual totals and monthly climatology in future years, as well as potential changes in drought metric and rainy season characteristics. At the annual scale, modest increases in total precipitation are projected, particularly under SSP2-4.5, with stronger signals in northern Florida. However, these increases are accompanied by enhanced intra-annual variability, especially during early summer, as reflected in higher coefficients of variation. Such changes indicate a growing likelihood of rainfall intermittency and cumulative deficits despite little change in annual means. Results also indicate intensification of rainfall deficits in future years, which is consistent with different models, although the degree of intensification slightly varies.

Regional contrasts further shape the projected impacts. Northern Florida is projected to experience consistent increases in annual and rainy-season rainfall with relatively modest rises in variability. By contrast, southern Florida, despite its higher baseline rainfall, exhibits stronger drying tendencies, heightened variability, and greater vulnerability to early-season deficits under SSP3-7.0. Central Florida presents mixed outcomes, reflecting considerable model spread. These differences highlight the inadequacy of uniform adaptation strategies and emphasize the need for region-specific planning. The RCD-based drought metrics point to southern Florida as particularly at risk, with larger increases in the frequency of critical rainfall deficit months. Furthermore, rainy-season projections suggest later onset dates and greater interannual variability, especially under the high-emission scenario during the latter half of the century (2056–2085).

From a management perspective, these results highlight the need for adaptive, climate-informed, and region-specific strategies. Existing infrastructure and allocation frameworks will be challenged by rising variability and more frequent droughts, requiring reservoir operations, storage, and preparedness plans to explicitly address cumulative deficits and seasonal unpredictability. One limitation of this study is its exclusive focus on precipitation. Potential changes in temperature, sea-level rise, and salinity intrusion, among other factors, may pose additional challenges for local water-resources management. Climate-resilient planning and management therefore require these drivers to be considered in an integrated and strategic manner. While the overall diagnostic workflow is broadly applicable, several elements (e.g., drought/deficit thresholds, rainy-season definitions, and deficit accumulation windows) are region- and application-specific. Application to other regions would therefore require locally appropriate re-definition and justification of these parameters, rather than direct transfer of the Florida-specific values used in this study.

Author Contributions

Hui Wang: conceptualization, methodology, data curation, formal analysis, visualisation, writing – original draft. **Tirusew Asefa:** conceptualization, methodology, visualisation, writing – review and editing. **Vasubandhu Misra:** methodology, visualisation, writing – review and editing.

Conflicts of Interest

The authors declare no conflicts of interest.

Data Availability Statement

All the data used in this work can be obtained without restriction. The NLDAS precipitation data is freely available from NOAA (https://hydro1.gesdisc.eosdis.nasa.gov/data/NLDAS/NLDAS_FORA0125_H.2.0/) and data from 18 CMIP6 General Circulation Models (GCMs) can be downloaded from the Earth System Grid Federation (ESGF) archives (https://esgf-node.llnl.gov/search/cmip6/).

References

Allan, R. P., M. Barlow, M. P. Byrne, et al. 2020. "Advances in Understanding Large-Scale Responses of the Water Cycle to Climate Change." *Annals of the New York Academy of Sciences* 1472, no. 1: 49–75.

Asadieh, B., and N. Y. Krakauer. 2015. "Global Trends in Extreme Precipitation: Climate Models Versus Observations." *Hydrology and Earth System Sciences* 19, no. 2: 877–891. https://doi.org/10.5194/hess-19-877-2015.

Asefa, T., and A. Adams. 2013. "Reducing Bias-Corrected Precipitation Projects Uncertainties: A Bayesian-Based Indicator Weighting Approach." *Regional Environmental Change* 13: 111–120. https://doi.org/10.1007/s10113-013-0431-9.

Chang, S., W. Graham, J. Geurink, N. Wanakule, and T. Asefa. 2018. "Evaluation of Impacts of Future Climate Change and Water Use Scenarios on Regional Hydrology." *Hydrology and Earth System Sciences* 22: 4793–4813. https://doi.org/10.5194/hess-22-4793-2018.

Eyring, V., S. Bony, G. A. Meehl, et al. 2016. "Overview of the Coupled Model Intercomparison Project Phase 6 (CMIP6) Experimental Design and Organization." *Geoscientific Model Development* 9, no. 5: 1937–1958. https://doi.org/10.5194/gmd-9-1937-2016.

Fischer, E., and R. Knutti. 2016. "Observed Heavy Precipitation Increase Confirms Theory and Early Models." *Nature Climate Change* 6: 986–991. https://doi.org/10.1038/nclimate3110.

Haarsma, R. J., M. J. Roberts, P. L. Vidale, et al. 2016. "High Resolution Model Intercomparison Project (HighResMIP v1.0) for CMIP6." *Geoscientific Model Development* 9, no. 11: 4185–4208. https://doi.org/10.5194/gmd-9-4185-2016.

Haasnoot, M., V. Di Fant, J. Kwakkel, and J. Lawrence. 2024. "Lessons From a Decade of Adaptive Pathways Studies for Climate Adaptation." *Global Environmental Change* 88: 102907. https://doi.org/10.1016/j.gloenvcha.2024.102907.

Hirabayashi, Y., R. Mahendran, S. Koirala, et al. 2013. "Global Flood Risk Under Climate Change." *Nature Climate Change* 3: 816–821. https://doi.org/10.1038/nclimate1911.

IPCC. 2021. *Climate Change 2021: The Physical Science Basis. Contribution of Working Group I to the Sixth Assessment Report of the Intergovernmental Panel on Climate Change*, edited by V. Masson-Delmotte, P. Zhai, A. Pirani, et al. Cambridge University Press. https://doi.org/10.1017/9781009157896.

Jones, E. R., M. F. P. Bierkens, and M. T. H. van Vliet. 2024. "Current and Future Global Water Scarcity Intensifies When Accounting for Surface Water Quality." *Nature Climate Change* 14: 629–635. https://doi.org/10.1038/s41558-024-02007-0.

Jung, H. 2025. "Groundwater Recharge in a Warming World." *Nature Climate Change* 15: 243. https://doi.org/10.1038/s41558-025-02286-1.

Kundzewicz, Z. W., L. J. Mata, N. W. Arnell, et al. 2007. "Freshwater Resources and Their Management." In *Climate Change 2007: Impacts, Adaptation and Vulnerability. Contribution of Working Group II to the Fourth Assessment Report of the Intergovernmental Panel on Climate Change*, edited by M. L. Parry, O. F. Canziani, J. P. Palutikof, P. J. van der Linden, and C. E. Hanson, 173–210. Cambridge University Press.

Lawrence, D. M., R. A. Fisher, C. D. Koven, et al. 2019. "The Community Land Model Version 5: Description of New Features, Benchmarking, and Impact of Forcing Uncertainty." *Journal of Advances in Modeling Earth Systems* 11: 4245–4287. https://doi.org/10.1029/2018MS001583.

Li, H., J. Sheffield, and E. F. Wood. 2010. "Bias Correction of Monthly Precipitation and Temperature Fields From Intergovernmental Panel on Climate Change AR4 Models Using Equidistant Quantile Matching." *Journal of Geophysical Research* 115: D10101. https://doi.org/10.1029/2009JD012882.

Li, W., L. Li, R. Fu, Y. Deng, and H. Wang. 2011. "Changes to the North Atlantic Subtropical High and Its Role in the Intensification of Summer Rainfall Variability in the Southeastern United States." *Journal of Climate* 24: 1499–1506. https://doi.org/10.1175/2010JCLI3829.1.

Li, Z., T. Liu, Y. Huang, J. Peng, and Y. Ling. 2022. "Evaluation of the CMIP6 Precipitation Simulations Over Global Land." *Earth's Future* 10, no. 8: e2021EF002500. https://doi.org/10.1029/2021EF002500.

Lobell, D. B., W. Schlenker, and J. Costa-Roberts. 2011. "Climate Trends and Global Crop Production Since 1980." *Science* 333, no. 6042: 616–620.

Lu, J., G. A. Vecchi, and T. Reichler. 2007. "Expansion of the Hadley Cell Under Global Warming." *Geophysical Research Letters* 34: L06805. https://doi.org/10.1029/2006GL028443.

Marella, R. L. 2008. *Water Withdrawals, Use, and Trends in Florida, 2005*. US Geological Survey. https://pubs.usgs.gov/publication/sir20095125.

Milly, P. C. D., J. Betancourt, M. Falkenmark, et al. 2008. "Stationarity Is Dead: Whither Water Management?" *Science* 319, no. 5863: 573–574.

Misra, V., A. Bhardwaj, and A. Mishra. 2018. "Characterizing the Rainy Season of Peninsular Florida." *Climate Dynamics* 51: 2157–2167. https://doi.org/10.1007/s00382-017-4005-2.

Misra, V., and S. DiNapoli. 2013. "Understanding Wet Season Variations Over Florida." *Climate Dynamics* 40: 1361–1372.

Mitchell, K. E., D. Lohmann, P. R. Houser, et al. 2004. "The Multi-Institution North American Land Data Assimilation System (NLDAS): Utilizing Multiple GCIP Products and the Eta Model Land Surface Scheme." *Journal of Geophysical Research: Atmospheres* 109, no. D7: D07S90. https://doi.org/10.1029/2003JD003823.

Nieto Ferreira, R., and T. M. Rickenbach. 2020. "Effects of the North Atlantic Subtropical High on Summertime Precipitation Organization in the Southeast United States." *International Journal of Climatology* 40, no. 14: 5987–6001. https://doi.org/10.1002/joc.6561.

Obeysekera, J., W. Graham, M. C. Sukop, et al. 2017. "Implications of Climate Change on Florida's Water Resources." In *Florida's Climate: Changes, Variations, and Impacts*, edited by E. P. Chassignet, J. W. Jones, V. Misra, and J. Obeysekera, 83–124. Florida Climate Institute.

O'Neill, B. C., C. Tebaldi, D. P. van Vuuren, et al. 2016. "The Scenario Model Intercomparison Project (ScenarioMIP) for CMIP6." *Geoscientific Model Development* 9, no. 9: 3461–3482. https://doi.org/10.5194/gmd-9-3461-2016.

Pendergrass, A. G., R. Knutti, F. Lehner, C. Deser, and B. M. Sanderson. 2017. "Precipitation Variability Increases in a Warmer Climate." *Scientific Reports* 7: 17966. https://doi.org/10.1038/s41598-017-17966-y.

Piao, S., P. Ciais, Y. Huang, et al. 2010. "The Impacts of Climate Change on Water Resources and Agriculture in China." *Nature* 467: 43–51. https://doi.org/10.1038/nature09364.

Polade, S. D., A. Gershunov, D. R. Cayan, M. D. Dettinger, and D. W. Pierce. 2017. "Precipitation in a Warming World: Assessing Projected Hydro-Climate Changes in California and Other Mediterranean Climate Regions." *Scientific Reports* 7: 10783. https://doi.org/10.1038/s41598-017-11285-y.

Riahi, K., D. P. van Vuuren, E. Kriegler, et al. 2017. "The Shared Socioeconomic Pathways and Their Energy, Land Use, and Greenhouse Gas Emissions Implications: An Overview." *Global Environmental Change* 42: 153–168. https://doi.org/10.1016/j.gloenvcha.2016.05.009.

Schewe, J., J. Heinke, D. Gerten, et al. 2014. "Multimodel Assessment of Water Scarcity Under Climate Change." *Proceedings of the National Academy of Sciences* 111, no. 9: 3245–3250.

Schmidt, D. F., and K. M. Grise. 2017. "The Response of Local Precipitation and Sea Level Pressure to Hadley Cell Expansion." *Geophysical Research Letters* 44, no. 20: 10573–10582. https://doi.org/10.1002/2017GL075380.

Schulzweida, U. 2022. "CDO User Guide (2.1.0). Zenodo." https://doi.org/10.5281/zenodo.7112925.

Seidel, D. J., Q. Fu, W. J. Randel, and T. J. Reichler. 2008. "Widening of the Tropical Belt in a Changing Climate." *Nature Geoscience* 1, no. 1: 21–24. https://doi.org/10.1038/ngeo.2007.38.

Srivastava, A., R. Grotjahn, and P. Ullrich. 2020. "Evaluation of Historical CMIP6 Model Simulations of Extreme Precipitation Over Contiguous US Regions." *Weather and Climate Extremes* 29: 100268. https://doi.org/10.1016/j.wace.2020.100268.

Swain, D. L., B. Langenbrunner, J. D. Neelin, and A. Hall. 2018. "Increasing Precipitation Volatility in Twenty-First-Century California." *Nature Climate Change* 8: 427–433. https://doi.org/10.1038/s41558-018-0140-y.

Swart, N. C., J. N. S. Cole, V. V. Kharin, et al. 2019. "The Canadian Earth System Model Version 5 (CanESM5.0.3)." *Geoscientific Model Development* 12, no. 11: 4823–4873. https://doi.org/10.5194/gmd-12-4823-2019.

Tebaldi, C., K. Hayhoe, J. M. Arblaster, and G. A. Meehl. 2006. "Going to the Extremes." *Climatic Change* 79: 185–211. https://doi.org/10.1007/s10584-006-9051-4.

Teutschbein, C., and J. Seibert. 2012. "Bias Correction of Regional Climate Model Simulations for Hydrological Climate-Change Impact Studies: Review and Evaluation of Different Methods." *Journal of Hydrology* 456: 12–29. https://doi.org/10.1016/j.jhydrol.2012.05.052.

Ukkola, A. M., M. G. De Kauwe, M. L. Roderick, G. Abramowitz, and A. J. Pitman. 2020. "Robust Future Changes in Meteorological Drought in CMIP6 Projections Despite Uncertainty in Precipitation." *Geophysical Research Letters* 47, no. 11: e2020GL087820. https://doi.org/10.1029/2020GL087820.

Wang, C., S.-K. Lee, and D. B. Enfield. 2008. "Climate Response to Anomalously Large and Small Atlantic Warm Pools During the Summer." *Journal of Climate* 21, no. 11: 2437–2450. https://doi.org/10.1175/2007JCLI2029.1.

Wang, H., and T. Asefa. 2024. "Enhanced Performance of CMIP6 Climate Models in Simulating Historical Precipitation in the Florida Peninsula." *International Journal of Climatology* 44, no. 8: 2758–2778. https://doi.org/10.1002/joc.8479.

Wang, H., T. Asefa, F. Getachew, and Y. Zhou. 2026. "Multi-Scale Shifts in Rainfall Patterns in a Subtropical Region (1981–2024): Challenges and Implications for Water Management." *Journal of Hydrology* 667: 134851. https://doi.org/10.1016/j.jhydrol.2025.134851.

Westra, S., H. J. Fowler, J. P. Evans, et al. 2014. "Future Changes to the Intensity and Frequency of Short-Duration Extreme Rainfall." *Reviews of Geophysics* 52, no. 3: 522–555.

Xia, Y., K. Mitchell, M. Ek, et al. 2012. "Continental-Scale Water and Energy Flux Analysis and Validation for the North American Land Data Assimilation System Project Phase 2 (NLDAS-2): 1. Intercomparison and Application of Model Products." *Journal of Geophysical Research: Atmospheres* 117, no. D3: D03109. https://doi.org/10.1029/2011JD016048.

Zhang, B., S. Song, H. Wang, et al. 2025. "Evaluation of the Performance of CMIP6 Models in Simulating Extreme Precipitation and Its Projected Changes in Global Climate Regions." *Natural Hazards* 121: 1737–1763. https://doi.org/10.1007/s11069-024-06850-4.

Zhao, J., T. Y. Gan, G. Zhang, and S. Zhang. 2023. "Projected Changes of Precipitation Extremes in North America Using CMIP6 Multi-Climate Model Ensembles." *Journal of Hydrology* 621: 129598. https://doi.org/10.1016/j.jhydrol.2023.129598.

Supporting Information

Additional supporting information can be found online in the Supporting Information section. **Data S1:** Supporting Information.